

UDC: 577.213:616.12

Alterations in lncRNAs H19 and TUG1 expression and their correlation with hemodynamics in myocardial infarction

M. Khetsuriani¹, T. I. Drevytska¹, L. V. Tumanovska¹, G. V. Portnichenko¹,
Y. Hegel-Valentych², V. O. Niekrasova³, A. M. Shysh¹, V. Dosenko¹

¹ Bogomoletz Institute of Physiology, National Academy of Sciences,
4, Bogomoletz Str., Kyiv, Ukraine, 01024

² Jagiellonian University, WBBiB,
24, Gołębia Str., Kraków, Poland, 31-007

³ Biology And Medicine Institute Science Educational Center Of Taras Shevchenko National University Of Kyiv,
2, Hlushkova Ave., Kyiv, Ukraine, 03022
khetsuriani@biph.kiev.ua

Aim. This study aimed to investigate the changes in hemodynamic parameters and expression of lncRNAs H19 and TUG1 in a rat model of myocardial infarction (MI). **Methods.** The effects of MI (ligating the LAD during 4 weeks) on the hemodynamic parameters were evaluated using a specific recording catheter. Additionally, we assessed the changes in myocardial and plasma levels of lncRNAs H19 and TUG1 using quantitative PCR. Pearson's correlation coefficient analysis was employed to understand the relationship between the lncRNAs expression and hemodynamic parameters. **Results.** Our study revealed significant alterations in several hemodynamic parameters post-MI. The expression levels of H19 significantly decreased, while TUG1 increased in the myocardium and blood plasma of rats following MI. A strong correlation was identified between these lncRNAs and several hemodynamic parameters. **Conclusions.** The data suggest that H19 and TUG1 are potentially important regulators of cardiac function post-MI, with their altered expression levels being associated with significant changes in key hemodynamic parameters. These findings underscore the importance of lncRNAs in the cardiac response to MI and pave the way for future studies to further elucidate their precise role and potential as therapeutic targets or biomarkers in heart disease.

Key words: H19, TUG1, long non-coding RNAs, myocardial infarction, hemodynamics, RNA.

© Institute of Molecular Biology and Genetics, NAS of Ukraine, 2023

© Publisher PH "Akademperiodyka" of the NAS of Ukraine, 2023

This is an Open Access article distributed under the terms of the Creative Commons Attribution License (<http://creativecommons.org/licenses/by/4.0/>), which permits unrestricted reuse, distribution, and reproduction in any medium, provided the original work is properly cited

Introduction

Cardiovascular diseases (CVDs) remain a leading cause of death worldwide, despite the significant advancements in medical science and technology [1]. Among these diseases, myocardial infarction (MI) or heart attack is particularly fatal and debilitating. Understanding the molecular mechanisms of MI is vital in developing effective diagnostic and therapeutic approaches.

In recent years, long non-coding RNAs (lncRNAs) have emerged as crucial components in the pathogenesis of various diseases, including CVDs [2]. lncRNAs are a class of transcripts longer than 200 nucleotides that do not encode proteins. Previously considered “transcriptional noise,” lncRNAs are now known to mediate numerous cellular functions, such as chromatin remodeling, transcriptional control, post-transcriptional processing, and intracellular trafficking [3].

Two such lncRNAs, H19 and TUG1, have been implicated in the cardiovascular field. H19, an imprinted gene product, is highly expressed in cardiac tissues and has been associated with the pathological processes of MI [4]. It has been found to play a role in cardiac fibrosis and hypertrophy, two significant events following MI, suggesting its influential role in cardiac pathophysiology.

Similarly, TUG1 (taurine upregulated gene 1) has been linked with cardiovascular diseases, specifically MI [5, 6]. The studies have shown that TUG1 can modulate cardiomyocyte apoptosis, a critical event in myocardial ischemia/reperfusion injury, indicating its potential as a target in the MI therapy.

However, despite the identified associations of H19 and TUG1 with cardiovascular diseases, particularly MI, many facets remain unexplored. For instance, their expression changes in MI and their correlation with hemodynamic parameters are not yet fully understood.

Therefore, this study was designed to investigate the changes in the expression of lncRNAs H19 and TUG1 in a rat model of myocardial infarction. We also sought to explore the correlation between the expression of these lncRNAs and the hemodynamic parameters, thereby adding to the growing body of knowledge on the role of lncRNAs in CVDs and potentially paving the way for novel diagnostic and therapeutic strategies.

Materials and methods

Animals

Adult male Wistar rats with 350–380 g body weight were obtained from the vivarium of A.A. Bogomoletz Institute of Physiology, NAS of Ukraine. The rats were divided into two groups of 9 animals each: the experimental group, which underwent an acute myocardial infarction (AMI) model, and the control group, which underwent a sham operation.

All study procedures were conducted in compliance with the EU directive 86/609/EEC and the ethical guidelines sanctioned by the Ethics Committee at the A.A. Bogomoletz Institute of Physiology, NAS of Ukraine.

Rat AMI model

Rats were anesthetized via an intraperitoneal injection of ketamine (0.8 mg/100 g). A special volume-controlled animal respirator was used to maintain the animals' respiration through a tracheal cannula. The heart was exposed through a left thoracotomy, followed by passing a 6–0 silk suture on a small curved needle through the myocardium underneath the left arterial descending (LAD) branch of the coronary artery. Myocardial ischemia was induced by ligating the LAD.

For the sham-operated group, the same procedure was carried out, but the suture was not tied. Four weeks post-surgery, the animals were euthanized and their hearts and blood plasma collected for the subsequent analysis.

Determining the level of fibrosis

To determine the development of fibrosis in the myocardium, we used Van Gieson staining for connective tissue. Frozen hearts were cut into 4 parts, each 3–4 mm thick (cross-sections), and then the thin frozen slices, 10–12 μm thick, were obtained from each part of the heart using a microtome. The slices were fixed in 96 % ethanol for 20 minutes and incubated in a saturated solution of picric acid for 1 hour. The following steps were then performed sequentially: incubation in a 0.5 % solution of glacial acetic acid for 10–30 seconds, incubation in a mixture of acidic fuchsin and a saturated solution of picric acid (1:10) for 1–2 minutes, rinsing in distilled water, and fixation in 96 % ethanol. The stained slices were scanned, and the resulting images were analyzed using the specialized morphometric software ImageJ (“National Institutes of Health”, USA).

Recording of hemodynamic parameters

The rats were anesthetized with urethane, secured, and the right carotid artery was prepared. A standard 2F pressure recording catheter (SPR-838; Millar Instruments, USA) was calibrated by volume by immersing it in a cuvette (P/N 910–1048) filled with heparinized rat blood.

The ultra miniature catheter was introduced retrogradely through the right carotid artery into the left ventricle (LV), allowing simultaneous recording of LV pressure and volume with visualization of the dependency curves of these parameters throughout the cardiac cycle.

The software ChartTM v.5.4.2 (ADInstruments, Millar Instruments, USA) was used to record hemodynamic parameters under conditions of a closed thoracic cavity [7]. The LV pressure-volume relationship was analyzed using the PVAN 3.6 software package (ADInstruments, Millar Instruments, USA). Calculations were made taking into account the initial and repeat catheter calibration values of the MPVS 400 Systems device. The basic real-time hemodynamic parameters were recorded, namely maximum and minimum pressure, heart rate (HR), LV volume, as well as the first derivative of pressure — dP/dt_{max} based on decoding the curves describing the pressure and volume dependence throughout each cardiac cycle.

The main hemodynamic indicators were grouped for convenience and, thus, pump function, diastolic function, contractility, pre- and afterload of the heart were analyzed. Conclusions were also made about the changes in the end-systolic (ESP) and end-diastolic pressure (EDP), end-systolic (ESV) and end-diastolic volume (EDV).

RNA extraction

The protocol used for RNA extraction from the samples involved a guanidine isothiocyanate-phenol-chloroform extraction method using Trizol reagent (Invitrogen). The extracted RNA was then diluted 50 times in dH₂O, and its concentration was determined with a Nano-Drop ND1000 spectrophotometer. To isolate total RNA from blood plasma, miR-39 was added at a concentration of 1 fM/1 μ l (miRNeasy Serum/Plasma Spike-In Control, Syn-cel-miR-39 miRNA, Lot No. 227926630, a product of the United States).

Reverse transcription

The process of reverse transcription was carried out in two stages. Initially, 6 μ l of total RNA were combined with 1 μ l of Random Hexamer Primer and 5 μ l of dH₂O. The samples were then incubated for 5 minutes at 70 °C in a GeneAmp® PCR System 2700 thermal cycler, Applied Biosystems (USA). Following this, 2 μ l of dNTP (x10), 4 μ l of Buffer RT, 0.5 μ l of RiboLock RNase inhibitor, and 0.9 μ l of Revert Aid RT (ThermoFisher Scientific, USA) were introduced to the samples. The samples were then incubated for 60 minutes at 42 °C, followed by 10 minutes at 70 °C. The reverse transcription of plasma RNA was carried out using specific loop primers for synthetic cel-miR-39 miRNA as a normalization control added before RNA extraction (miR Neasy Serum/Plasma Spike-In Control, Syn-cel-miR-39 miRNA, Lot No. 227926630, USA).

Quantitative real-time PCR

A 7500 Fast Real-Time PCR thermal cycler by Applied Biosystems (USA) and a 96-well

plate were employed for qPCR. The utilized mix consisted of 5 μ l of SybrGreen max, 2 μ l of cDNA, 0.08 μ l of specific primers for rat H19 and TUG1, 0.2 μ l of Rox (1:9), and 2.72 μ l of H₂O, resulting in a final reaction volume of 10 μ l. DNA denaturation was carried out at 95 °C for 15 seconds. The annealing and elongation of probes were conducted at 60 °C for 1 minute, and the number of cycles was set at 50.

The specific sequences for the primers used in the real-time RT-PCR are provided below: H19 forward — 5'-GCACAGGATGAAGCCAGACAAGG-3', H19 reverse — 5'-TCTCCGAGACACCGATCACTGC-3'; TUG1 forward — 5'-ACAGTTTCCCTCTACCCAGTG-3'; TUG1 reverse — 5'-GCCTATGTCAA ACTTTGCCCA-3'; beta-actin forward (reference gene) — 5'-CTTGCAGCTCCTCCGTCGCC-3'; beta-actin reverse (reference gene) — 5'-CTTGCTCTGGGCCTCCTCGTCGC-3'.

The level of relative expression was calculated using the $2^{-\Delta\Delta CT}$ method, where $\Delta\Delta CT = \Delta CT$ (a target sample) – ΔCT (a reference sample).

Statistical analysis

Statistical analysis was carried out using a t-test, assuming the data followed a normal distribution (as confirmed by the Shapiro-Wilk test) and equal variances (as confirmed by the Levene's test). In the cases where these conditions were not met, the Mann-Whitney test was utilized for analysis. The changes in lncRNAs expression were evaluated with a one-way ANOVA test. The correlation analysis between lncRNAs expression and hemodynamic parameters was estimated using Pearson correlation coefficient.

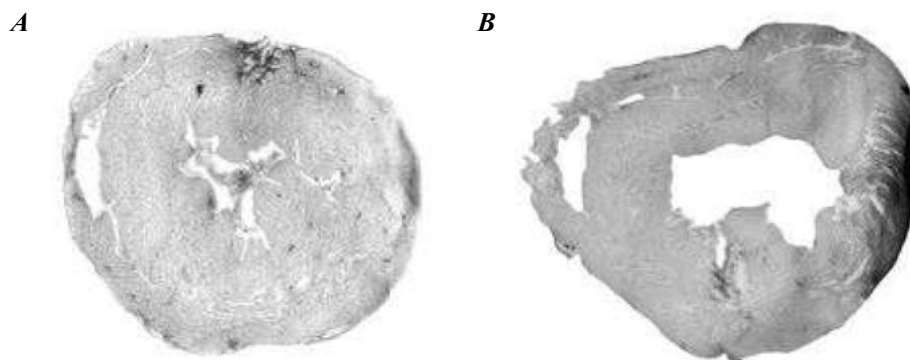


Fig. 1. Slices of rat heart stained using the Van Gieson method: *A* — SHAM; *B* — AMI.

A p-value less than 0.05 was deemed statistically significant.

Results and Discussion

Hemodynamic parameters

To confirm myocardial infarction, we determined the level of cardiac fibrosis using the described method (Fig. 1). According to our findings, the average fibrosis level in the hearts of AMI group rats was $13.2\% \pm 1.28$. In the SHAM group, this value was $3.4\% \pm 0.31$. Thus, the fibrosis area in the AMI rat group was almost four times larger than in the SHAM group.

The effects of MI on hemodynamic parameters are complex, reflecting both the direct impact of the loss of myocardial tissue and the compensatory mechanisms that the body deploys in response (Tab. 1).

According to the data obtained, in the AMI group, we observed a deterioration in diastolic and systolic functions. This is indicated by a significant increase in the end-systolic volume (ESV), end-diastolic volume (EDV) and end-diastolic pressure (EDP) in AMI rats ($p < 0.05$). This is consistent with the develop-

ment of post-MI ventricular remodeling, a process characterized by dilatation of the ventricle and increased volumes [8–10].

The ESP indicator also increased, but this is not significant ($p > 0.05$). The Tau W parameter in AMI rats significantly increases (from 7.06 to 10.49 msec), indicating an increase in relaxation time during infarction. A deterioration in systolic heart function is also indicated by a significant decrease in dV/dt_{max} , preload adjusted maximal power parameters ($p < 0.05$), as well as a decrease in cardiac output, although this parameter decreased insignificantly ($p > 0.05$) [11, 12]. The arterial stiffness indicator in rats of the AMI group surprisingly significantly decreased from 0.47 to 0.32 mmHg/ μ L ($p < 0.05$), which remains unclear to us. Insignificant changes in cardiac output and decreasing arterial stiffness might occur as a compensatory response to maintain blood flow following myocardial infarction [13, 14].

H19 and TUG1 expression in myocardium

We analyzed the expression of long non-coding RNAs (lncRNAs) H19 and TUG1 in the myocardium, as well as in the plasma of rats in both groups. The analysis of the results showed that the level of lncRNA H19 expres-

Table 1. Main hemodynamic parameters in rats with SHAM surgery and an AMI model (values are mean \pm SEM)

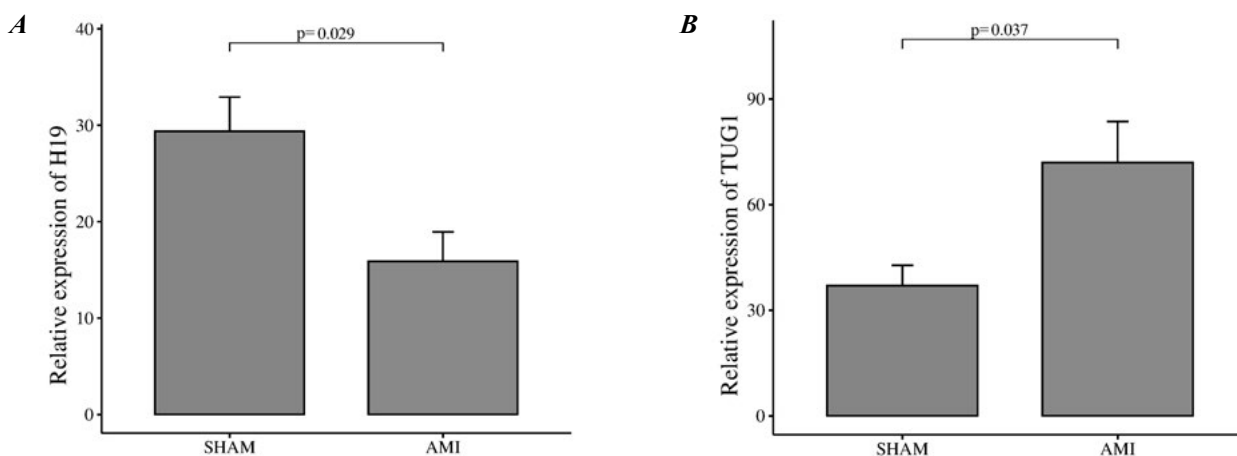
Parameter	SHAM group (n = 9)	AMI group (n = 9)
Heart rate (bpm)	322.89 \pm 39.6	323.33 \pm 22.62
End-systolic Volume (μ L)	210.87 \pm 18.74	303.63 \pm 39.83*
End-diastolic Volume (μ L)	377.96 \pm 47.98	537.9 \pm 35.34*
End-systolic Pressure (mmHg)	88.22 \pm 8.52	94.88 \pm 5.97
End-diastolic Pressure (mmHg)	2.07 \pm 2.17	8.13 \pm 1.51*
Stroke Volume (μ L)	219.47 \pm 20.4	234.94 \pm 19.69
Ejection Fraction (%)	50.93 \pm 2.52	53.29 \pm 3.24
Cardiac Output (μ L/min)	74766.21 \pm 6332.87	68149.4 \pm 9932.8
Stroke Work (mmHg* μ L)	16187.33 \pm 2537.83	17629.67 \pm 2334.41
Arterial Elastance (Ea) (mmHg/ μ L)	0.47 \pm 0.06	0.32 \pm 0.02*
dP/dt _{max} (mmHg/sec)	9556.56 \pm 1269.88	9582 \pm 1712.99
dP/dt _{min} (mmHg/sec)	-7013.11 \pm 436.15	-6116 \pm 552.67
dV/dt _{max} (μ L/sec)	17312 \pm 2879.34	13239.89 \pm 2512.24*
dV/dt _{min} (μ L/sec)	-12490.7 \pm 1611.54	-11365.8 \pm 1470.14
Tau W (msec)	7.04 \pm 1.04	10.49 \pm 0.56*
Preload adjusted maximal power (mWatts/ μ L ²)	8.26 \pm 1.78	3.26 \pm 0.26*

* p < 0.05

sion in the myocardium drops almost twofold in rats from the AMI group (p<0.05) (Fig. 2).

Numerous studies have already been published demonstrating the cardioprotective

properties of lncRNA H19, therefore, its decrease in the myocardial infarction model was predictable. Specifically, in the study by Wang H *et al.*, it was demonstrated how

**Fig. 2.** H19 (a) and TUG1 (b) myocardial expression in Wistar rats with AMI model.

lncRNA H19 suppresses cardiac hypertrophy by sponging microRNA-145 [15]. Gong LC *et al.* showed that lncRNA H19 protects cardiomyocytes from hypoxia-induced injury [16]. This effect is achieved through the activation of the PI3K/AKT and ERK/p38 pathways, which are important for protecting myocardial cells against ischemic injury. In the study by Zhang L *et al.*, it was demonstrated that overexpression of H19 slows down the apoptosis of cardiomyocytes in neonatal rats [17]. An experiment with mice demonstrated that H19 has protective properties for the heart during myocardial infarction by activating autophagy through upregulating the ratio of LC3-II/I and the expressions of Beclin-1 and ATG-7 [18].

Noteworthy, the cardioprotective properties of H19 are still a subject of discussion. This long non-coding RNA can be involved in various pathways, and each specific case is a subject for deep study. For example, in the study by Tao H *et al.*, a molecular mechanism was proposed in which lncRNA H19 promotes the development of fibrosis in heart tissues [19]. In the study by Choong OK *et al.*, it was shown that H19 can form a nucleoprotein complex with Y box-binding protein (YB-1) under hypoxia, which induces fibrosis and cardiac remodeling after infarction [20].

Given the significant decrease in the level of H19 in our myocardial infarction model, we suggest that H19 overexpression (as a variant of RNA therapy) could improve the hemodynamic indicators of animals and also reduce the level of post-infarction fibrosis.

As for lncRNA TUG1, its expression was almost twice as high in the rats from the AMI group. This likely indicates the involvement

of lncRNA TUG1 in the development of the pathological process in the heart.

Possibly, interference with this lncRNA will contribute to the normalization of hemodynamic parameters of the post-infarction heart, as well as the reduction of fibrosis. This is also indicated by a number of other studies. In the study by Su Q *et al.*, it was shown that TUG1 mediates ischemic myocardial injury by sponging miR-132 [21]. Wang YW *et al.* demonstrated that transcription factor HIF-1 α binds to the promoter region of TUG1 up-regulating its expression in cardiomyocytes during hypoxia/reoxygenation [5]. In this study it was demonstrated that the detrimental effect of TUG1 is caused by its direct interaction with the FUS (fused in sarcoma) protein, which is involved in cardiac repair after MI. Fu D *et al.* showed that TUG1 enhances the apoptosis of cardiomyocytes in ischemia-reperfusion myocardial injury [22]. And through sponging microRNA 29b-3p and miR-34a, TUG1 contributes to cardiac hypertrophy [23, 24].

H19 and TUG1 levels in plasma

We also analyzed the levels of lncRNAs H19 and TUG1 in the blood plasma of rats from both groups. The level of H19 expression in the plasma significantly drops 2.42-fold ($p < 0.01$) (Fig. 3). Meanwhile, the level of TUG1 increases insignificantly by 46.7 % ($p > 0.05$).

These results suggest that lncRNA H19 can be considered as a potential marker for ischemic heart damage. At the same time, a number of questions remain open. For example, does the decrease in the expression of lncRNA H19 in the blood plasma relate to its decreased

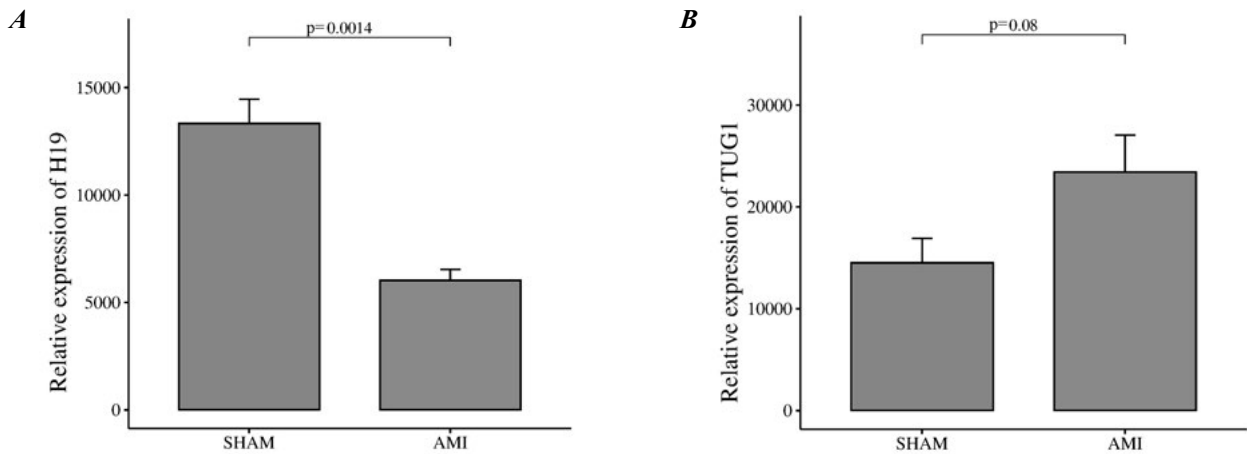


Fig. 3. H19 (a) and TUG1 (b) plasma expression in Wistar rats with AMI model.

level in the myocardium, since H19 is not a cardio-specific long non-coding RNA.

Correlation analysis between hemodynamic parameters and the expression level of H19 and TUG1

In this study, we employed the Pearson’s correlation coefficient analysis to assess the linear

relationship between specific hemodynamic parameters and the expression levels of lncRNAs H19 and TUG1 in a rat model of AMI (Fig. 4).

For lncRNA H19, the expression levels showed a moderate positive correlation with ESP ($r = 0.59$) and TauW ($r = 0.64$), and a strong positive correlation with dP/dtmax

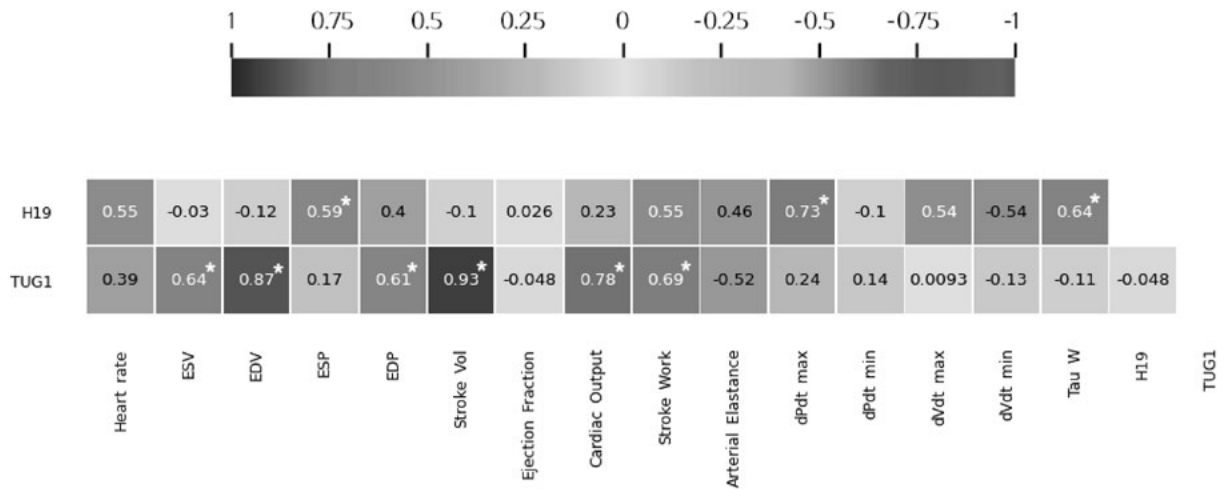


Fig. 4. Correlation matrix of hemodynamic parameters and lncRNAs H19 and TUG1 expression levels in AMI rat model (* $p < 0.05$)

($r = 0.73$). This suggests that the expression of H19 may be associated with systolic function and the rate of left ventricular pressure rise and fall, implying a potential role in contractility and relaxation following AMI.

For lncRNA TUG1, there were strong positive correlations with more measured parameters. The highest correlation was observed with stroke volume ($r = 0.93$), indicating that TUG1 expression may strongly associate with the volume of blood pumped out of the heart per beat in the AMI model. Similarly, EDV, a measure of the total amount of blood in the heart at the end of diastole, also showed a very strong positive correlation ($r = 0.87$). The correlations with cardiac output ($r = 0.78$) and stroke work ($r = 0.69$), indicate a possible association of TUG1 expression with the overall function and workload of the heart in AMI conditions.

These findings suggest that both H19 and TUG1 could potentially serve as important regulators of cardiac function post-AMI, either directly influencing these hemodynamic parameters or being regulated in response to their changes. However, further research is needed to elucidate the exact mechanisms of their involvement and to explore their potential as therapeutic targets in AMI.

Conclusion

In conclusion, our study provides valuable insights into the intricate hemodynamic changes and molecular responses in a rat model of AMI. We observed significant alterations in several hemodynamic parameters following MI, including increased end-systolic and end-diastolic volumes, stroke volume, cardiac output, and stroke work. Additionally, we noted

a significant decrease in arterial elastance and the maximal rate of volume change during systole, dV/dt_{max} .

At the molecular level, we demonstrated that the expression of lncRNAs H19 and TUG1, which have been implicated in various cardiac pathological processes, significantly changes in both the myocardium and blood plasma following MI. Specifically, we reported a significant decrease in H19 and an increase in TUG1 expression. Furthermore, our correlation analysis revealed strong associations between these lncRNAs and various hemodynamic parameters, potentially suggesting a crucial role for H19 and TUG1 in the cardiac response to MI.

Though our results highlight the potential of H19 and TUG1 as markers for ischemic heart damage and their potential roles in modulating hemodynamic parameters following MI, several questions remain open. Future studies are warranted to elucidate the exact mechanisms by which these lncRNAs influence cardiac function following MI, and whether these lncRNAs could serve as effective therapeutic targets or biomarkers for the diagnosis, prognosis, or treatment of ischemic heart disease. This study underscores the complex interplay between molecular and physiological responses to myocardial infarction and represents an important step forward in our understanding of the pathophysiology of this disease.

REFERENCES

1. *Mc Namara K, Alzubaidi H, Jackson JK. Cardiovascular disease as a leading cause of death: how are pharmacists getting involved? Integr Pharm Res Pract. 2019; 8:1–11.*

2. Fang Y, Xu Y, Wang R, *et al.*, and Zhang M. Recent advances on the roles of lncRNAs in cardiovascular disease. *J Cell Mol Med.* 2020; **24**(21):12246–57.
3. Quinn JJ, Chang HY. Unique features of long non-coding RNA biogenesis and function. *Nat Rev Genet.* 2016; **17**(1):47–62.
4. Busscher D, Boon RA, Juni RP. The multifaceted actions of the lncRNA H19 in cardiovascular biology and diseases. *Clin Sci (Lond).* 2022; **136**(15):1157–78.
5. Wang YW, Dong HZ, Tan YX, *et al.*, and Su Q. HIF-1 α -regulated lncRNA-TUG1 promotes mitochondrial dysfunction and pyroptosis by directly binding to FUS in myocardial infarction. *Cell Death Discov.* 2022; **8**(1):178.
6. Su Q, Liu Y, Lv XW, *et al.*, and Kong BH. lncRNA TUG1 mediates ischemic myocardial injury by targeting miR-132–3p/HDAC3 axis. *Am J Physiol Heart Circ Physiol.* 2020; **318**(2):H332–H344.
7. Pacher P, Nagayama T, Mukhopadhyay P, *et al.*, and Kass DA. Measurement of cardiac function using pressure-volume conductance catheter technique in mice and rats. *Nat Protoc.* 2008; **3**(9):1422–34.
8. Pfeffer MA, Braunwald E. Ventricular remodeling after myocardial infarction. *Experimental observations and clinical implications.* *Circulation.* 1990; **81**(4):1161–72.
9. Cohn JN, Ferrari R, Sharpe N. Cardiac remodeling—concepts and clinical implications: a consensus paper from an international forum on cardiac remodeling. Behalf of an International Forum on Cardiac Remodeling. *J Am Coll Cardiol.* 2000; **35**(3):569–82.
10. Sutton MG, Sharpe N. Left ventricular remodeling after myocardial infarction: pathophysiology and therapy. *Circulation.* 2000; **101**(25):2981–8.
11. Pacher P, Nagayama T, Mukhopadhyay P, *et al.*, and Kass DA. Measurement of cardiac function using pressure-volume conductance catheter technique in mice and rats. *Nat Protoc.* 2008; **3**(9):1422–34.
12. Schmidt MR, Smerup M, Konstantinov IE, *et al.*, and Kharbanda RK. Intermittent peripheral tissue ischemia during coronary ischemia reduces myocardial infarction through a KATP-dependent mechanism: first demonstration of remote ischemic preconditioning. *Am J Physiol Heart Circ Physiol.* 2007; **292**(4):H1883–90.
13. Opie LH, Commerford PJ, Gersh BJ, Pfeffer MA. Controversies in ventricular remodelling. *Lancet.* 2006; **367**(9507):356–67.
14. Kelly RP, Ting CT, Yang TM, *et al.*, and Kass DA. Effective arterial elastance as index of arterial vascular load in humans. *Circulation.* 1992; **86**(2):513–21.
15. Wang H, Lian X, Gao W, *et al.*, and Wang L. Long noncoding RNA H19 suppresses cardiac hypertrophy through the MicroRNA-145–3p/SMAD4 axis. *Bioengineered.* 2022; **13**(2):3826–39.
16. Gong LC, Xu HM, Guo GL, *et al.*, and Chang C. Long Non-Coding RNA H19 Protects H9c2 Cells against Hypoxia-Induced Injury by Targeting MicroRNA-139. *Cell Physiol Biochem.* 2017; **44**(3):857–69.
17. Zhang L, Liu T, Wang P, *et al.*, and Huang T. Overexpression of Long Noncoding RNA H19 Inhibits Cardiomyocyte Apoptosis in Neonatal Rats with Hypoxic-Ischemic Brain Damage Through the miR-149–5p/LIF/PI3K/Akt Axis. *Biopreserv Biobank.* 2021; **19**(5):376–85.
18. Zhou M, Zou YG, Xue YZ, *et al.*, and Zhang Q. Long non-coding RNA H19 protects acute myocardial infarction through activating autophagy in mice. *Eur Rev Med Pharmacol Sci.* 2018; **22**(17):5647–51.
19. Tao H, Cao W, Yang JJ, *et al.*, and Li J. Long non-coding RNA H19 controls DUSP5/ERK1/2 axis in cardiac fibroblast proliferation and fibrosis. *Cardiovasc Pathol.* 2016; **25**(5):381–9.
20. Choong OK, Chen CY, Zhang J, *et al.*, and Hsieh PCH. Hypoxia-induced H19/YB-1 cascade modulates cardiac remodeling after infarction. *Theranostics.* 2019; **9**(22):6550–67.
21. Su Q, Liu Y, Lv XW, *et al.*, and Kong BH. lncRNA TUG1 mediates ischemic myocardial injury by targeting miR-132–3p/HDAC3 axis. *Am J Physiol Heart Circ Physiol.* 2020; **318**(2):H332–H344.
22. Fu D, Gao T, Liu M, *et al.*, and Fu X. lncRNA TUG1 aggravates cardiomyocyte apoptosis and myocardial ischemia/reperfusion injury. *Histol Histopathol.* 2021; **36**(12):1261–72.
23. Zou X, Wang J, Tang L, Wen Q. lncRNA TUG1 contributes to cardiac hypertrophy via regulating miR-29b-3p. *In Vitro Cell Dev Biol Anim.* 2019; **55**(7):482–90.

24. Fang Q, Liu T, Yu C, et al., and Zou X. LncRNA TUG1 alleviates cardiac hypertrophy by targeting miR-34a/DKK1/Wnt- β -catenin signalling. *J Cell Mol Med.* 2020; **24**(6):3678–91.

Зміни в експресії lncRNAs H19 та TUG1 та їх кореляція з гемодинамікою при інфаркті міокарда

М. Хецуріані, Т. І. Древицька, Л. В. Тумановська, Г. В. Портніченко, Й. Гегель-Валентичь, В. О. Некрасова, А. М. Шиш, В. Є. Досенко

Мета. Метою цього дослідження було дослідити зміни гемодинамічних параметрів і експресії lncRNAs H19 та TUG1 у моделі інфаркту міокарда (ІМ) у щурів. **Методи.** Вплив ІМ (лігатура на лівій коронарній артерії протягом 4 тижнів) на гемодинамічні параметри було оцінено за допомогою спеціального катетера для запису. Додатково ми оцінювали зміни у рівнях lncRNAs H19 та TUG1 у міокарді і плазмі крові за допомогою кількісного ПЦР. Кореляційний аналіз із коефіцієнтом Пірсона був використаний для визна-

чення взаємозв'язку між експресією цих lncRNAs та гемодинамічними параметрами. **Результати.** Було виявлено значні зміни у декількох гемодинамічних параметрах після ІМ. Рівні експресії H19 значно знизилися, тоді як TUG1 збільшилася в міокарді і плазмі крові щурів після ІМ. Достовірна кореляція була встановлена між цими lncRNAs та декількома гемодинамічними параметрами. **Висновки.** Дані свідчать про те, що H19 та TUG1 є потенційно важливими регуляторами функції серця після ІМ, а зміни їх експресії асоціюються із значними змінами ключових гемодинамічних параметрів. Це підкреслює важливість lncRNAs при МІ та відкривають шлях для майбутніх досліджень, спрямованих на подальше вивчення їх точної ролі та потенціалу як терапевтичних мішеней або біомаркерів при серцевих патологіях.

Ключові слова: H19, TUG1, довгі некодуючі РНК, інфаркт міокарда, гемодинаміка, РНК.

Received 19.06.2023